

## Admittance measurements of acceptor freezeout and impurity conduction in Be-doped GaAs

T. W. Hickmott

*IBM Research Division, Thomas J. Watson Research Center, Yorktown Heights, New York 10598*

(Received 28 June 1991)

Carrier freezeout and impurity conduction in lightly doped  $p$ -type GaAs have been studied in two groups of  $p^-$ -type GaAs—undoped  $\text{Al}_x\text{Ga}_{1-x}\text{As}$ — $p^+$ -type GaAs capacitors. For one group the substrate doping was  $N_S \sim 5 \times 10^{14} \text{ cm}^{-3}$ ; for the other  $N_S \sim 5 \times 10^{15} \text{ cm}^{-3}$ . From the temperature dependence of the appearance of a Gray-Brown dip in the capacitance-voltage curves at fixed frequency and temperature, the separation of the Be acceptor from the valence band,  $E_A$ , is  $\sim 20 \text{ meV}$  for both groups. The activation energy for ac transport in  $p^-$ -type GaAs,  $E_I$ , is determined from admittance measurements at fixed bias and variable temperature and frequency. For the lighter-doped samples,  $E_I = 17\text{--}23 \text{ meV}$ , which is consistent with the value of  $E_A$ . For the heavier-doped samples,  $E_I \sim 6 \text{ meV}$ ; ac transport is either through a well-defined impurity band separated by  $\sim 6 \text{ meV}$  from the energy level of an isolated acceptor, or by activated hopping.

### INTRODUCTION

Impurity conduction in lightly doped semiconductors at low temperatures, i.e., conduction through localized impurity states, has been studied for many years.<sup>1–3</sup> It is closely bound up with the question of how conduction can occur in semiconductors when donors or acceptors are separated by distances that are large compared to the Bohr radius of the impurity and the sample temperature is so low that carriers are not excited into the conduction or valence band. The occurrence of impurity conduction depends on the presence of compensating minority impurities; for  $p$ -type semiconductors with  $N_A$  acceptors/cm<sup>3</sup>, impurity conduction depends on the presence of  $N_D$  donors/cm<sup>3</sup> with  $N_A > N_D$ . Impurity conduction can occur for a wide range of the compensation ratio  $K = N_D/N_A$ . Hall-effect measurements as a function of temperature are customarily used to determine  $N_A$ ,  $N_D$ , and the activation energies for acceptor impurities  $E_A$  and for donor impurities  $E_D$ . One characteristic feature of impurity conduction is that semiconductor resistivity varies much more rapidly than linearly with impurity concentration. A second characteristic is that the majority-carrier Hall mobility is unmeasurably small. At low temperatures, sample resistance is measured in the impurity conduction or hopping regime, but carrier concentration and mobility are not determined separately. Impurity conduction has been studied over a wide concentration range in  $p$ -type Ge (Refs. 4 and 5) and  $p$ -type Si,<sup>6</sup> as well as in  $n$ -type GaAs.<sup>7,8</sup> Impurity conduction has been reported in Zn-doped GaAs (Ref. 9) and in ion-implanted Be-doped GaAs (Ref. 10) at carrier concentrations greater than  $10^{18} \text{ cm}^{-3}$ , and in Cd-doped and Zn-doped GaAs with  $N_A$  greater than  $1 \times 10^{17} \text{ cm}^{-3}$ .<sup>11</sup> However, there are no reports of impurity conduction in lightly doped  $p$ -type GaAs nor are there measurements for temperatures  $T \lesssim 30 \text{ K}$ .

Beryllium is commonly used as a  $p$ -type dopant in GaAs heterostructures grown by molecular-beam epitaxy

(MBE).<sup>12,13</sup> Its ease of evaporation and its low vapor pressure at the growth temperatures make it possible to obtain hole concentrations greater than  $10^{19} \text{ cm}^{-3}$ . The energy separation of a Be acceptor from the valence band of GaAs,  $E_A$ , is 28 meV from optical measurements.<sup>14</sup> In general, activation energies measured thermally are less than those measured optically. Values of  $E_A$  for Be in GaAs from the temperature dependence of Hall measurements have been reported as 15,<sup>13</sup> 24–32,<sup>15</sup> and 5 meV.<sup>10</sup> There is an ambiguity in analyzing Hall measurements; whether one measures  $E_A$  or  $E_A/2$  depends on compensation, which is difficult to determine.<sup>16</sup> Measurements on samples with doping less than  $10^{17} \text{ cm}^{-3}$  are difficult below about 30 K because the sample resistance becomes too large.

Admittance spectroscopy, in which one measures the frequency and temperature dependence of the capacitance and conductance of semiconductor capacitors or diodes, has been extensively used to measure semiconductor properties. It is most commonly used to measure deep levels in semiconductors,<sup>17–20</sup> interface states in metal-oxide-semiconductor (MOS) capacitors,<sup>21–23</sup> or heterostructure band offsets.<sup>24</sup> Aymeloglu and Zemel<sup>25</sup> used admittance measurements on MOS field-effect transistors to measure activation energies for freezeout of donors in  $n$ -type silicon at temperatures between 14 and 26 K.

In the present paper, capacitance-voltage ( $C$ - $V$ ) and admittance measurements on  $p^-$ -type GaAs—undoped  $\text{Al}_x\text{Ga}_{1-x}\text{As}$ — $p^+$ -type GaAs ( $\text{Al}_x\text{Ga}_{1-x}\text{As}$ ) capacitors are used to measure the activation energy for freezeout of conduction in lightly doped  $p$ -type GaAs. Samples with very thin (0.6  $\mu\text{m}$ ) active regions are used. This makes it possible to study freezeout in lightly doped materials that are inaccessible to Hall measurements, since the total sample resistance at a given temperature is significantly less than that of a Hall sample, which typically has dimensions of several hundred  $\mu\text{m}$ . From the measured values of  $E_A$  we conclude that impurity conduction can

occur in  $p$ -type GaAs at carrier concentrations as low as  $5 \times 10^{15} \text{ cm}^{-3}$ .

### EXPERIMENT

The semiconductor-insulator-semiconductor ( $S$ - $I$ - $S$ ) capacitor used to study freezeout in  $p$ -type GaAs is the  $p$ -type GaAs-undoped  $\text{Al}_x\text{Ga}_{1-x}\text{As}$ - $p$ -type GaAs heterostructure shown schematically in the energy diagram of Fig. 1(a).<sup>26</sup> The  $\text{Al}_x\text{Ga}_{1-x}\text{As}$  capacitor was grown by MBE on a heavily doped,  $\langle 100 \rangle$ -oriented,  $p$ -type GaAs wafer. Be was the  $p$ -type dopant. A  $p$ -type GaAs buffer layer  $\sim 200$  nm thick was first grown, followed by a  $p$ -type GaAs layer  $\sim 600$  nm thick with substrate concentration  $N_S = N_A - N_D$ . The undoped  $\text{Al}_x\text{Ga}_{1-x}\text{As}$  layer of thickness  $w$  was grown and was followed by a 300-nm heavily doped gate layer with an acceptor concentration  $N_G$ , which was graded to a surface layer with  $1 \times 10^{19} \text{ cm}^{-3}$  Be doping for better Ohmic contacts. The Be source was off while  $\sim 3$  nm on either side of the  $\text{Al}_x\text{Ga}_{1-x}\text{As}$  layer was grown. After sample growth Ohmic Ag-Zn contacts were made to the  $p$ -type GaAs wafer and to the  $p$ -type GaAs gate. Gold films were used as an etch mask to form  $S$ - $I$ - $S$  capacitors of  $4 \times 10^{-4} \text{ cm}^2$  area. Samples were mounted in TO-5 headers for low-temperature measurements.

When a  $p$ -type  $\text{Al}_x\text{Ga}_{1-x}\text{As}$  capacitor is biased by a negative gate voltage  $V_G$ , a hole accumulation layer forms on the  $p$ -type GaAs substrate, as shown in Fig. 1(a).  $V_G$  has three components;  $\psi_S$  is the band bending in the substrate,  $\psi_G$  is the band bending in the gate, and  $V_I$  is the voltage drop across the insulating  $\text{Al}_x\text{Ga}_{1-x}\text{As}$  layer.  $\phi_h$ , the activation energy for the emission of holes over the  $\text{Al}_x\text{Ga}_{1-x}\text{As}$  barrier at the  $p$ -type GaAs/ $\text{Al}_x\text{Ga}_{1-x}\text{As}$  interface, is determined from the temperature dependence of current-voltage ( $I$ - $V$ ) curves in the temperature range 100–250 K, in which thermionic emission dominates the  $I$ - $V$  curves.<sup>27,28</sup> Table I lists parameters for the samples used in the present work.  $N_S$  and  $N_G$  are determined from  $C$ - $V$  curves, as has been done for  $n$ -type  $\text{Al}_x\text{Ga}_{1-x}\text{As}$  capacitors.<sup>27</sup>

If the  $p$ -type  $\text{Al}_x\text{Ga}_{1-x}\text{As}$  capacitor is biased into accumulation, as in Fig. 1(a), the equivalent circuit of Fig. 1(b) is an excellent representation. At constant  $V_G$  the capacitance

$$\frac{1}{C_T} = \frac{1}{C_S} + \frac{1}{C_I} + \frac{1}{C_G} \quad (1)$$

TABLE I. Properties of  $\text{Al}_x\text{Ga}_{1-x}\text{As}$  capacitors.  $x$  is the AlAs mole fraction in  $\text{Al}_x\text{Ga}_{1-x}\text{As}$ ;  $N_S$  is the substrate doping;  $N_G$  is the gate doping;  $w_{cp}$  is the  $\text{Al}_x\text{Ga}_{1-x}\text{As}$  thickness from  $C$ - $V$  measurements;  $\epsilon_I$  is the  $\text{Al}_x\text{Ga}_{1-x}\text{As}$  dielectric constant for modeling  $C$ - $V$  curves;  $V_{FB}$  is the measured flat-band voltage;  $\phi_h$  is the activation energy for thermionic emission of holes;  $d$  is the thickness of  $p$ -type GaAs calculated from admittance measurements.

Sample	$x$	$N_S$ ( $10^{15} \text{ cm}^{-3}$ )	$N_G$ ( $10^{18} \text{ cm}^{-3}$ )	$w_{cp}$ (nm)	$\epsilon_I$	$V_{FB}$ (V)	$\phi_h$ (eV)	$d$ ( $\mu\text{m}$ )
A	0.4	0.4–0.7	0.7	36.0	11.2	0.0	0.213	0.55
B	0.3	0.4–0.7	0.3	50.0	11.8	0.0	0.167	0.51
C	0.5	0.4–0.7	0.8	26.0	10.9	0.0	0.259	0.54
D	0.6	4–6	1.5	31.0	10.6	0.0	0.30	0.56
E	0.5	4–6	0.8	47.5	10.9	−0.085	0.325	0.53

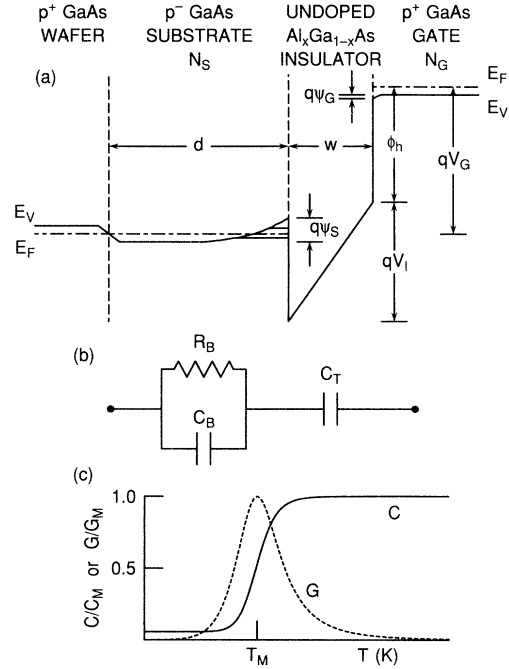


FIG. 1. (a) Schematic energy-band diagram for  $p$ -type GaAs-undoped  $\text{Al}_x\text{Ga}_{1-x}\text{As}$ - $p$ -type GaAs ( $\text{Al}_x\text{Ga}_{1-x}\text{As}$ ) capacitor biased into accumulation. (b) Equivalent circuit representation for admittance of  $\text{Al}_x\text{Ga}_{1-x}\text{As}$  capacitor in accumulation. (c) Temperature dependence of parallel capacitance and conductance of the equivalent circuit of (b) calculated from Eqs. (2), (3), and (5).

is constant, where  $C_S$ ,  $C_I$ , and  $C_G$  are the capacitances of the accumulated substrate, the insulating  $\text{Al}_x\text{Ga}_{1-x}\text{As}$  layer, and the gate, respectively.  $C_I = \epsilon_I \epsilon_0 A / w$ , where  $\epsilon_I$  is the dielectric constant of the  $\text{Al}_x\text{Ga}_{1-x}\text{As}$  insulator,  $\epsilon_0$  is the permittivity of free space, and  $A$  is the sample area. Following Aymeloglu and Zemel,<sup>25</sup> in the freezeout regime at low temperatures the lightly doped substrate is represented by a parallel resistance  $R_B$  and capacitance  $C_B$ . If one measures the admittance of the  $S$ - $I$ - $S$  capacitor of Fig. 1(a) as a parallel capacitance  $C_P$  and a conductance  $G_P$  at an angular frequency  $\omega = 2\pi\nu$ , where  $\nu$  is the measurement frequency, then

$$\frac{C_P}{C_M} = \frac{1}{1 + \omega^2 (C_T + C_B)^2 R_B^2}, \quad (2)$$

$$\frac{G_P}{G_M} = \frac{2\omega(C_T + C_B)R_B}{1 + \omega^2(C_T + C_B)^2 R_B^2}, \quad (3)$$

where  $G_M$  is the maximum value of conductance and  $C_M = C_T$  is the maximum value of capacitance. The substrate capacitance is

$$C_B = \frac{\epsilon_S \epsilon_0 A}{d}, \quad (4)$$

where  $\epsilon_S$  is the dielectric constant of GaAs and  $d$  is the thickness of lightly doped  $p^-$ -type GaAs. As temperature decreases and the substrate freezes out, the resistance can be expressed as

$$R_B = R_0 e^{E_I/kT}. \quad (5)$$

$R_0$  is related to the resistance at high temperature,  $E_I$  is an ionization energy, and  $k$  is Boltzmann's constant. If one defines a time

$$\tau_R = (C_T + C_B)R_B, \quad (6)$$

then  $G_P$  has a maximum and  $C_P/C_M = 0.5$  when  $\omega\tau_R = 1$ .  $(C_T + C_B)$  is essentially constant in the temperature range where freezeout occurs; only  $\epsilon_S$  and  $\epsilon_I$  depend on temperature, and their change over the temperature range for acceptor freezeout is small. Equations (2) and (3) are equivalent to equations for Debye relaxation curves; they are plotted schematically in Fig. 1(c). At low temperatures  $C/C_M$  becomes constant. If  $f$  is the value of  $C/C_M$  in this temperature range,

$$C_B = \frac{fC_M}{(1-f)}. \quad (7)$$

Combining Eqs. (4) and (7), one can obtain a value of the effective thickness  $d$  of the  $p^-$ -type GaAs substrate in which freezeout occurs. By measuring the admittance of an  $\text{Al}_x\text{Ga}_{1-x}\text{As}$  capacitor as a function of temperature at different frequencies, a set of curves such as those of Fig. 1(c) is obtained, with  $T_M$  different for each frequency.  $E_I$  is determined from an Arrhenius plot of the logarithm of  $\omega$  as a function of  $1/T_M$ .

Admittance measurements were made on  $p$ -type  $\text{Al}_x\text{Ga}_{1-x}\text{As}$  capacitors using an HP 4274A LCR meter, which measures  $C_P$  and  $G_P$  directly. The ac modulation amplitude was 0.004 V rms. The impedance of the capacitor can equally well be represented by an equivalent circuit of a capacitance  $C_S$  in series with a resistor  $R_S$ .  $C_S$  and  $R_S$  are obtained from  $G_P$  and  $C_P$  by the formulas

$$C_S = (1 + D^2)C_P, \quad (8)$$

$$R_S = \frac{D^2}{(1 + D^2)G_P}, \quad (9)$$

where

$$D = \frac{G_P}{\omega C_P} = \omega R_S C_S \quad (10)$$

is the dissipation factor.  $R_S$  depends primarily on the resistivity of the  $p^-$ -type GaAs layer.

Measurement procedures for  $C$ - $V$  curves have been described.<sup>27,29</sup> For admittance measurements, the  $\text{Al}_x\text{Ga}_{1-x}\text{As}$  capacitor was held at constant temperature and gate voltage, while the frequency was varied. Seven frequencies between 1 and 100 kHz were used. The measurement voltage was then changed and the frequency cycle was repeated. Typically, 14–16 voltages were measured at a given temperature. For temperatures between 4.2 and 70 K, the sample holder was placed in a liquid-helium storage Dewar, above the liquid-helium level. The sample temperature was controlled and measured by two Lakeshore model DT-500 silicon diodes, which were close to the sample. A Lakeshore model DRC-80C controller regulated power to a 15-W heater in a copper block in which the TO-5 header with the sample was mounted. Temperatures were held constant to better than 0.1 K during measurements. A Lakeshore silicon diode mounted on a TO-5 header and calibrated against NIST standards between 1.6 and 100 K was substituted for the sample to determine the relation between sample temperature and the reading of the silicon diodes close to the sample. Temperatures have been corrected to agree with the calibrated silicon diode.

## RESULTS

The determination of activation energies from admittance measurements requires the determination of capacitance and conductance of an  $\text{Al}_x\text{Ga}_{1-x}\text{As}$  capacitor as a function of both temperature and frequency. Figure 2 shows typical  $C$ - $V$  and  $G$ - $V$  curves of sample *A* at 26 K and 100 kHz; it illustrates essential features that are observed for all the samples. For  $V_G \gtrsim 0.0$  V, the capacitance is small due to the formation of a depletion region

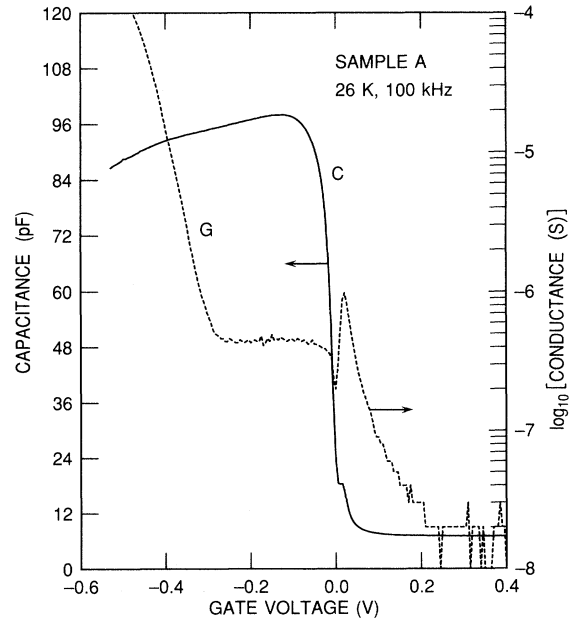


FIG. 2. Capacitance-voltage and conductance-voltage curves of sample *A* at 26 K and 100 kHz.

in the  $p^-$ -type GaAs substrate. For  $V_G \lesssim -0.1$  V the capacitance reaches a maximum and then decreases gradually. This is the voltage range illustrated schematically in Fig. 1(a), in which an accumulation layer forms on the  $p^-$ -type GaAs substrate. The gradual decrease in capacitance is due to depletion and band bending in the  $p^+$ -type GaAs gate. A characteristic feature of  $C$ - $V$  curves of  $p^-$ -type  $\text{Al}_x\text{Ga}_{1-x}\text{As}$  capacitors when freezeout of acceptors occurs is a Gray-Brown (GB) dip at  $\sim 0.0$  V.<sup>29,30</sup> The dip occurs when the temperature is such that the Fermi level in the lightly doped substrate is close to the acceptor level of the substrate dopant. At flat-band voltage  $V_{\text{FB}}$ , modulation of the occupancy of the acceptor level at the  $p^-$ -type GaAs/ $\text{Al}_x\text{Ga}_{1-x}\text{As}$  interface by the ac signal contributes an additional capacitance term  $C_F$ , so that the total measured capacitance is

$$\frac{1}{C_T} = \frac{1}{C_S} + \frac{1}{C_I} + \frac{1}{C_G} + \frac{1}{C_F}. \quad (11)$$

The observation of a GB dip in  $C$ - $V$  curves is one of the best ways of determining  $V_{\text{FB}}$  of an  $S$ - $I$ - $S$  capacitor. The dip occurs for all measurement frequencies.

The  $G$ - $V$  curve of Fig. 2 also has several characteristic features. Proceeding from depletion to accumulation, for  $V_G \gtrsim 0.2$  V,  $G$  is very small. An increase in  $G$  as  $V_G$  decreases is followed by an abrupt drop corresponding to the occurrence of a GB dip in capacitance. There is a plateau region of nearly constant  $G$  when the capacitor is biased in accumulation. A steep increase of  $G$  then occurs when current due to tunneling of holes through the  $\text{Al}_x\text{Ga}_{1-x}\text{As}$  barrier dominates ac conductance. The maximum voltage to measure  $G$  and  $C$  is determined by  $G$  becoming so large that the quality factor  $Q=1/D$  becomes less than 0.01. Admittance measurements have been made in the range  $-0.3 \lesssim V_G \lesssim -0.1$  V in which  $G$  is constant. As the temperature decreases, the value of  $G$  in the plateau region increases, reaches a maximum that depends on frequency, and then decreases.

Capacitance-voltage curves in depletion are used to determine the concentration profile of Be acceptors in the  $p^-$ -type GaAs substrate.<sup>31</sup> Carrier concentration as a function of depth below the  $\text{Al}_x\text{Ga}_{1-x}\text{As}/p^-$ -type GaAs interface is shown in Fig. 3 for five samples.  $C$ - $V$  curves used were measured at 77 K and 1 MHz. Strictly speaking, the acceptor concentration is not measured; the carrier concentration that is measured is  $N_A - N_D$ .  $N_D$  is not known for any of the samples. If similar curves are measured for  $T > 77$  K, the carrier concentrations are slightly higher, showing that some hole freezeout occurs even at 77 K. However, the major reduction in carrier concentration due to freezeout occurs below 30 K. The concentration profiles rise steeply below 100 nm;  $C$ - $V$  profiling close to the interface shows a rapid increase of carriers, which reflects the formation of the accumulation layer rather than the acceptor concentration. The two groups of samples differ by an order of magnitude in their concentrations. The assumption of constant substrate doping, which is made for purposes of modeling  $C$ - $V$  curves, is not true for any of the samples. Values of  $N_S$  given in Table I are approximate.

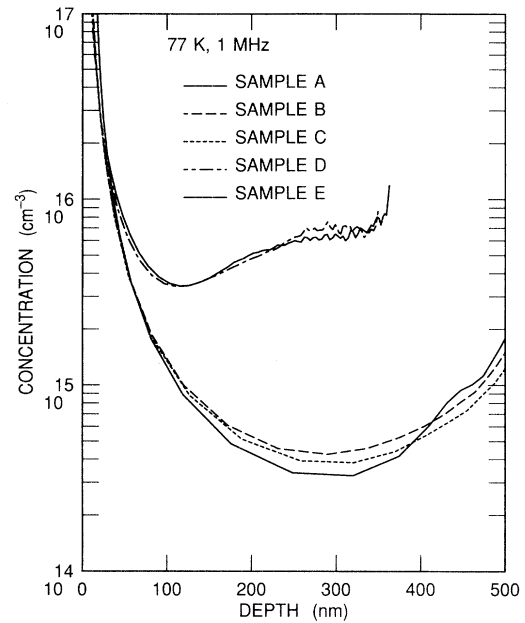


FIG. 3. Carrier concentration profiles for different samples, derived from  $C$ - $V$  curves at 77 K and 1 MHz.

Capacitance-voltage curves for  $S$ - $I$ - $S$  capacitors using  $\text{Al}_x\text{Ga}_{1-x}\text{As}$  as the dielectric are nearly ideal. For  $n^-$ -type  $\text{Al}_x\text{Ga}_{1-x}\text{As}$  capacitors, the density of surface states at the  $n^-$ -type GaAs/ $\text{Al}_x\text{Ga}_{1-x}\text{As}$  interface is  $< 2 \times 10^{10} \text{ cm}^{-2} \text{ eV}^{-1}$ ;<sup>27</sup> the density at the  $p^-$ -type GaAs/ $\text{Al}_x\text{Ga}_{1-x}\text{As}$  interface has not been measured, but there is no reason to expect it to be any larger, since GaAs and  $\text{Al}_x\text{Ga}_{1-x}\text{As}$  are closely lattice matched for all values of  $x$ . Computer programs that have been used to match experimental  $C$ - $V$  curves of  $n^-$ -type  $\text{Al}_x\text{Ga}_{1-x}\text{As}$  capacitors have been used to model  $p^-$ -type  $\text{Al}_x\text{Ga}_{1-x}\text{As}$  capacitors;<sup>32,33</sup> the values of  $N_S$ ,  $N_G$ , and  $w$  in Table I are derived from such matching of experimental and calculated  $C$ - $V$  curves. For  $n^-$ -type  $\text{Al}_x\text{Ga}_{1-x}\text{As}$  capacitors, no thermal freezeout of donors occurs at temperatures as low as 1.6 K, so in modeling  $C$ - $V$  curves the donor energy has been set equal to zero.<sup>32</sup> For  $p^-$ -type  $\text{Al}_x\text{Ga}_{1-x}\text{As}$  capacitors, inclusion of an acceptor energy in the model results in a GB dip in calculated  $C$ - $V$  curves. In Fig. 4, calculated  $C$ - $V$  curves are plotted for a capacitor with semiconductor parameters that approximate those of sample A and for different temperatures; only the voltage region close to  $V_{\text{FB}}$  is plotted in order to emphasize the development of a GB dip. The curves are shifted by 0.050 V on the voltage scale for clarity, but all curves are plotted to the same scale. In Fig. 4(a),  $E_A = 0.028$  eV, which is the optical value for Be in GaAs. A GB dip just begins to develop by 46–48 K. For  $E_A = 0.020$  eV structure at  $V_{\text{FB}}$  appears at 36–38 K with a well-developed minimum at 30 K. For  $E_A = 0.010$  eV there is an inflection at  $V_{\text{FB}}$  for the 20-K curve with a minimum resolved at 16 K. Thus lower values of  $E_A$  shift the appearance of a GB dip in calculated  $C$ - $V$  curves to lower

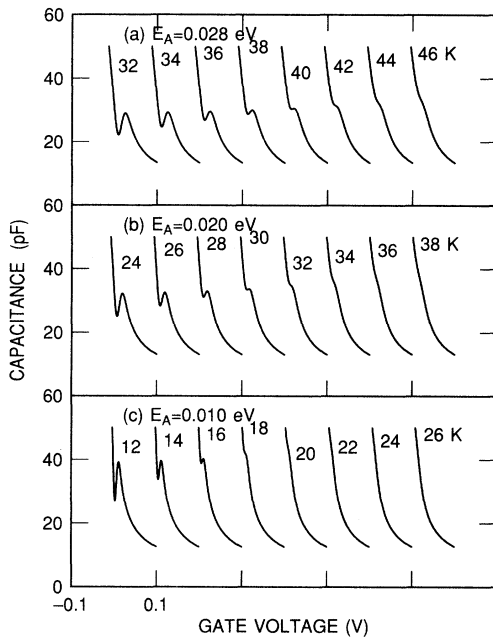


FIG. 4. Calculated  $C$ - $V$  curves for  $p$ -type  $\text{Al}_x\text{Ga}_{1-x}\text{As}$  capacitor at different temperatures for different values of acceptor activation energy  $E_A$ . Parameters for calculation:  $N_A = 1.0 \times 10^{15} \text{ cm}^{-3}$ ,  $N_D = 1.0 \times 10^{13} \text{ cm}^{-3}$ ,  $N_G = 1.0 \times 10^{18} \text{ cm}^{-3}$ ,  $\omega = 36 \text{ nm}$ ,  $\epsilon_r = 11.2$ , area =  $4.0 \times 10^{-4} \text{ cm}^2$ . All curves are on the same scale but are shifted by 0.050 V on the abscissa.

temperatures. Because of the heavier hole mass compared to the electron mass in GaAs,  $p$ -type GaAs is barely degenerate at  $N_G \sim 1 \times 10^{18} \text{ cm}^{-3}$  and 30 K. If an acceptor level and a small amount of compensation is included in both substrate and gate for calculated  $C$ - $V$  curves,  $V_{\text{FB}} \sim 0 \text{ V}$ . Values of  $V_{\text{FB}}$  in Table I are 0.0 V except for sample E, which has positive charge in the  $\text{Al}_x\text{Ga}_{1-x}\text{As}$  dielectric.

In Figs. 5(b) and 5(c),  $C$ - $V$  curves close to  $V_{\text{FB}}$  are plotted for samples A and D. For both samples structure at  $V_{\text{FB}}$  can be detected at 34–36 K, and a well-defined inflection is observed at 28–30 K. For comparison, calculated curves with  $E_A = 0.020 \text{ eV}$  are shown in Fig. 5(a). The appearance of structure at  $V_{\text{FB}}$  occurs at the same temperatures, 34–36 K, as for the experimental curves. Comparison of calculated and experimental curves is qualitative, but it indicates that the acceptor energy responsible for a GB dip is about the same in samples A and D; the activation energy is close to 0.020 eV.

Admittance measurements for sample A are shown in Fig. 6 and for sample D in Fig. 7. In each case,  $C/C_M$  or  $G/G_M$  is plotted as a function of temperature for different frequencies at a constant value of  $V_G$  in accumulation.  $C_M$  and  $G_M$  are the experimental maximum values of capacitance and conductance at each frequency and bias. The curves are nearly ideal Debye-like relaxation curves, as shown in Fig. 1(c). In each case,  $G/G_M$  is a maximum at the temperature at which  $C/C_M = 0.5$ . Values of  $G_M$  for different frequencies are proportional to

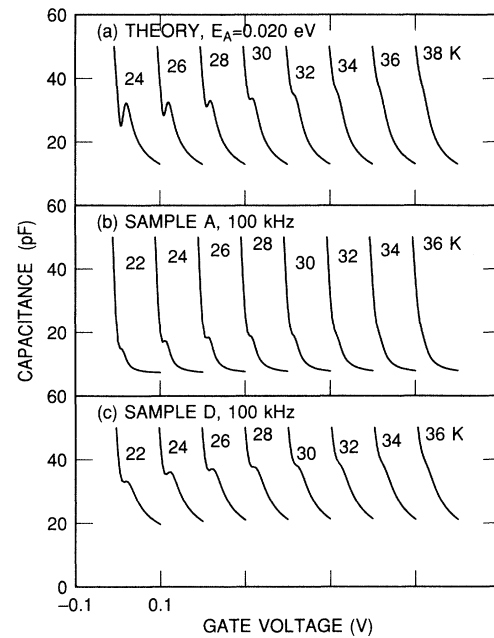


FIG. 5. (a) Calculated  $C$ - $V$  curves for  $p$ -type  $\text{Al}_x\text{Ga}_{1-x}\text{As}$  capacitor at different temperatures for  $E_A = 0.020 \text{ eV}$ . Parameters for the calculation are the same as in Fig. 4. (b) and (c) show experimental  $C$ - $V$  curves around 0 V for samples A and D at different temperatures. All curves are on the same scale but are shifted by 0.050 V on the abscissa.

$\omega$ , in accord with Eq. (3). The striking difference between the two samples is that the curves are shifted to significantly lower temperatures for sample D as compared to sample A.

Activation energies are obtained by plotting the logarithm of  $\omega$  as a function of  $1/T_M$ , where  $T_M$  is the temperature for the maximum in the conductance curve at frequency  $\omega$  for a given  $V_G$ . Figure 8 shows typical plots for each of the five samples. Activation energies given for each sample are least-squares fits of the five highest-frequency points, since these are more accurate than measurements at 1 and 3 kHz. The low-frequency points lie close to the lines. In Fig. 9 the activation energies for each sample are plotted as a function of  $V_G$  for the range of  $V_G$  in accumulation for which conductance at constant temperature is constant, as shown in Fig. 2. The vertical lines for each point show the standard deviation of the values of  $E_I$ . Activation energies for each sample are constant. Samples with low values of  $N_S$  fall in one group, samples with high values of  $N_S$  in the other. For sample A,  $E_I$  is  $\sim 23 \text{ meV}$ , which approaches the optical value for a Be acceptor in GaAs, 28 meV. Values of activation energies from temperature-dependent measurements are nearly always lower than values obtained from optical measurements, as is the case here.<sup>34</sup> Values of  $E_I$  for samples A, B, and C vary, although their substrate acceptor concentrations are nearly equal. Activation energies for the second group of samples D and E are markedly lower, which is consistent with the shift of admittance curves to lower temperatures in Fig. 7.

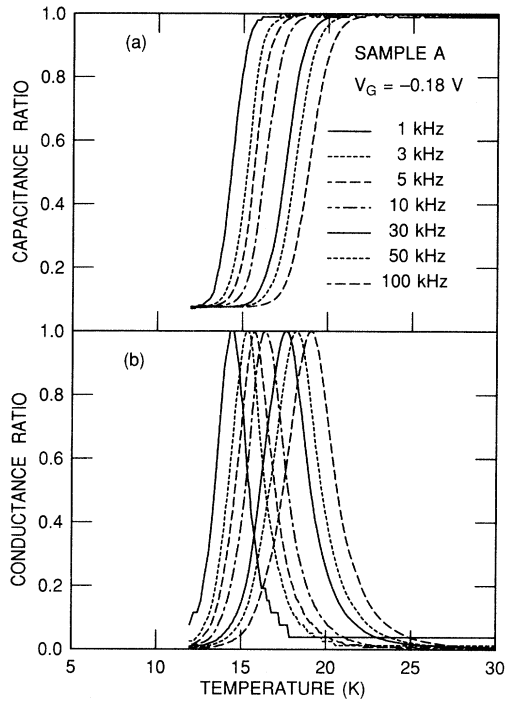


FIG. 6. Admittance plots for sample *A*.  $V_G = -0.18$  V. (a)  $C_P/C_M$  at different frequencies as a function of temperature.  $C_M = 97.5$  pF. (b)  $G_P/G_M$  at different frequencies as a function of temperature.  $G_M = 2.6 \times 10^{-7}$ ,  $7.8 \times 10^{-7}$ ,  $1.3 \times 10^{-6}$ ,  $2.6 \times 10^{-6}$ ,  $7.8 \times 10^{-6}$ ,  $1.3 \times 10^{-5}$ , and  $2.6 \times 10^{-5}$  S for  $\nu = 1-100$  kHz.

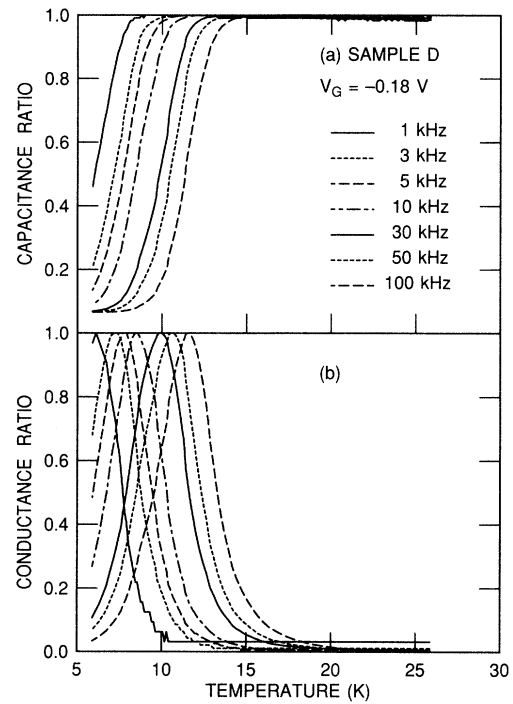


FIG. 7. Admittance plots for sample *D*.  $V_G = -0.18$  V. (a)  $C_P/C_M$  at different frequencies as a function of temperature.  $C_M = 114.5$  pF. (b)  $G_P/G_M$  at different frequencies as a function of temperature.  $G_M = 3.2 \times 10^{-7}$ ,  $9.4 \times 10^{-7}$ ,  $1.6 \times 10^{-6}$ ,  $3.1 \times 10^{-6}$ ,  $9.2 \times 10^{-6}$ ,  $1.5 \times 10^{-5}$ , and  $3.0 \times 10^{-5}$  S for  $\nu = 1-100$  kHz.

Conductance curves of  $G/G_M$  as a function of temperature, such as in Fig. 1(c), are symmetrical about  $T_M$ . For any value of  $G/G_M$ , there are two values of  $\omega\tau_R$  and therefore of  $T$  that satisfy Eq. (3). If  $T_L$  is the lower temperature and  $T_H$  is the higher temperature, and if the resistance is given by Eq. (5), then

$$\frac{T_H T_L}{T_H - T_L} = \frac{E_I}{kF \left[ \frac{G}{G_M} \right]} = P \left[ \frac{G}{G_M} \right], \quad (12)$$

where  $F(G/G_M)$  is the natural logarithm of the ratio of the two roots of Eq. (3) for the given value of  $G/G_M$ . If  $T_L = T_M - \Delta$  and  $T_H = T_M + \Delta$ , Eq. (12) can be used to calculate  $\Delta$ :

$$\Delta \left[ \frac{G}{G_M} \right] = -P + (P^2 + T_M^2)^{1/2}. \quad (13)$$

The shape of ideal conductance curves can be calculated from Eqs. (12) and (13) using experimental values of  $E_I$  and  $T_M$ . Figure 10 shows conductance curves at 10 and 100 kHz for four of the samples at  $V_G = -0.18$  V. The points are calculated from Eqs. (12) and (13). The experimental curves are nearly ideal Debye curves; in some cases they are slightly narrower than calculated curves, in other cases they are slightly broader, but in general there

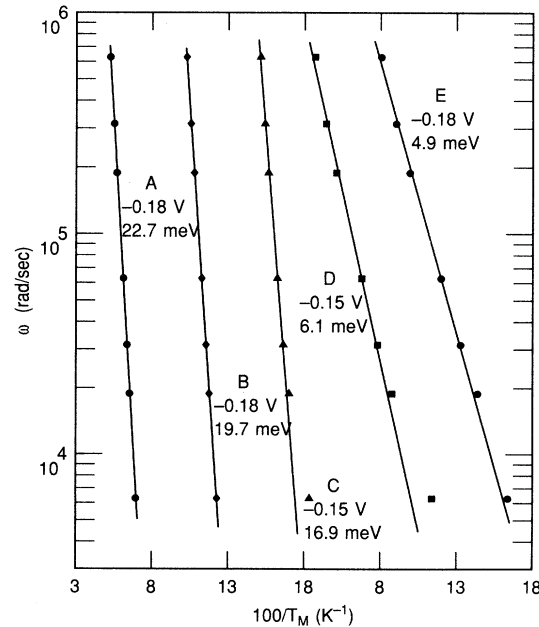


FIG. 8. Arrhenius plot of  $\omega$  vs  $1/T_M$  at constant  $V_G$  for different *p*-type  $\text{Al}_x\text{Ga}_{1-x}\text{As}$  capacitors. Curves are shifted on abscissa. Activation energies use five highest-frequency points.

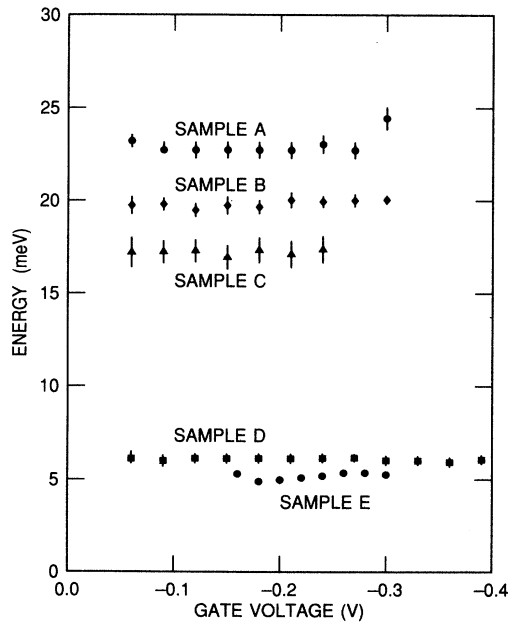


FIG. 9. Dependence of activation energy from admittance measurements on  $V_G$  in accumulation for different samples.

is close agreement between calculated conductance curves and experimental curves.

At low temperatures,  $C/C_M$  in Figs. 6 and 7 decreases to a constant value  $f$ . Equations (4) and (7) can be used to calculate an effective thickness  $d$  for the  $p^-$ -type GaAs substrate whose freezeout is responsible for the increase

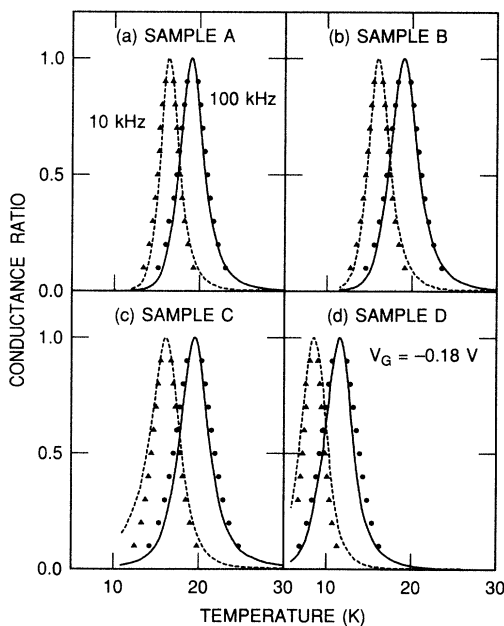


FIG. 10. Experimental conductance ratio curves at 10 and 100 kHz as a function of temperature.  $V_G = -0.18$  V. Points are calculated for ideal admittance curves from Eqs. (12) and (13).

in  $R_B$ . Values of  $d$  are given in Table I for each of the samples, using  $\epsilon_S = 12.6$ . Nominal values of  $d$  from growth times are  $0.6 \mu\text{m}$ ; experimental values are smaller. Some of the discrepancy is accounted for by the width of the accumulation layer, some by diffusion of Be from the heavily doped buffer layer into  $p^-$ -type GaAs, which gives a gradual change in carrier concentration at the contact between two  $p$ -type GaAs regions.

Admittance measurements on  $p$ -type  $\text{Al}_x\text{Ga}_{1-x}\text{As}$  capacitors have been made as a parallel capacitance  $C_p$  and conductance  $G_p$ . The series equivalent circuit given by Eqs. (8)–(10) is equally valid; it provides a way to check the validity of Eqs. (5) and (6), which are used to calculate  $E_I$ . Figure 11 shows  $R_S$  at 100 kHz as a function of  $1/T$  for four samples.<sup>29</sup> The curves are all on the same  $1/T$  scale but are shifted horizontally for clarity. Derivation of an activation energy from admittance curves using Eq. (6) assumes that resistance depends exponentially on  $1/T$ . The approximation is good for samples *A*, *B*, and *C*. The solid line is a least-squares fit according to Eq. (5); activation energies are obtained from plots of  $\log R_S$  as a function of  $1/T$ . The arrows for each curve show the temperature corresponding to the maximum in conductance curves for each sample. For samples *D* and *E* there is curvature in plots of  $\log R_S$  versus  $1/T$ . Activation energies are derived from the higher-temperature points in each case rather than from all the points below the maximum. Values of activation energy as a function of  $V_G$  for all five samples are shown in Fig.

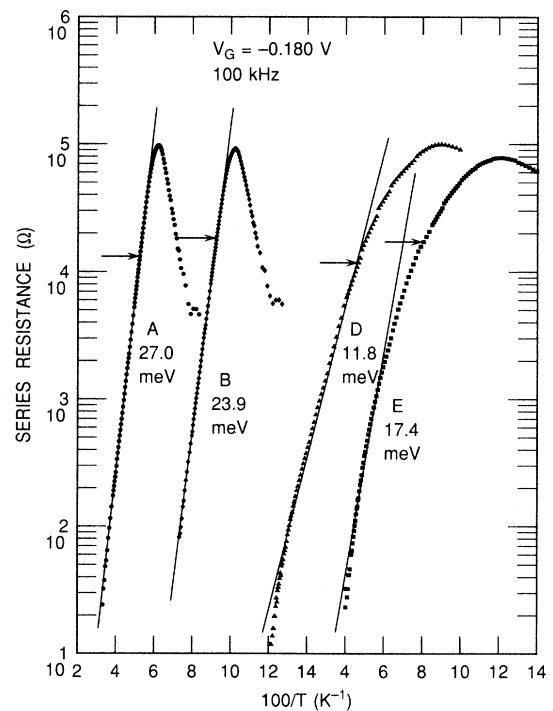


FIG. 11. Dependence of series resistance of  $p^-$ -type GaAs on  $1/T$  for four samples. Solid lines are least-squares fit of highest temperature points. Arrows show  $T_M$  for conductance ratio curves.

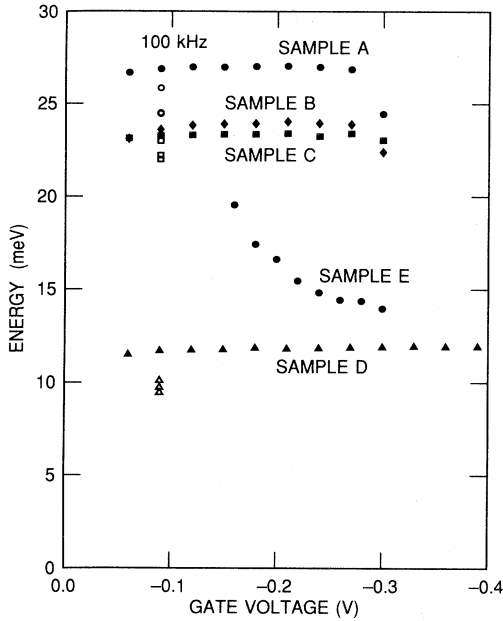


FIG. 12. Dependence of activation energy from series resistance measurements at 100 kHz on  $V_G$  for different samples. Open points show  $E_A$  at  $V_G = -0.09$  V at 50, 30, and 10 kHz for samples *A*, *C*, and *D*.

12. The solid points are for measurements at 100 kHz. For samples *A*, *C*, and *D*, the open points at  $-0.090$  V are activation energies at 50, 30, and 10 kHz, to show the range of values for a given sample. Activation energies from resistance for samples *A*, *B*, and *C* are higher than  $E_I$  from admittance measurements but are constant with  $V_G$ . For sample *E*, the values of activation energy vary with  $V_G$  reflecting the curvature that appears in Fig. 11. In general, Eq. (5) is satisfied over a range of temperatures around  $T_M$  for all samples, but a simple exponential dependence of  $R_S$  on  $1/T$  is not found for samples *D* and *E*.

## DISCUSSION

Admittance measurements and  $C$ - $V$  curves on  $p$ -type  $\text{Al}_x\text{Ga}_{1-x}\text{As}$  capacitors provide two activation energies for conduction in  $p$ -type GaAs. The activation energy from  $C$ - $V$  curves is the ionization energy of the Be acceptors in GaAs,  $E_A$ ; the activation energy from admittance measurements  $E_I$  is the activation energy for ac transport in  $p$ -type GaAs. From Fig. 5,  $C$ - $V$  curves for both groups of samples of different doping show the appearance of a GB dip in  $C$ - $V$  curves at  $\sim 34$ – $36$  K, with a well-developed dip at 28 K. Comparison with calculated  $C$ - $V$  curves shows that this corresponds to a separation of  $\sim 20$  meV between the acceptor level and the valence band. Admittance measurements give activation energies of 17–23 meV for samples with substrate doping  $(4$ – $7) \times 10^{14} \text{ cm}^{-3}$ , and energies of 5–6 meV for samples with  $N_S = (4$ – $6) \times 10^{15} \text{ cm}^{-3}$ . Activation energies from

$C$ - $V$  curves are estimated, but comparison with Fig. 4(c) shows clearly that the acceptor level is greater than 10 meV from the valence band in sample *D*.

Activation energies from admittance measurements are obtained from Arrhenius plots of  $\log \omega$  versus  $1/T_M$ . This is consistent with Eq. (5), which is the simplest phenomenological representation of an exponential dependence of  $R_B$  on temperature. Aymeloglu and Zemel<sup>25</sup> discuss a model of freezeout in a compensated semiconductor, from which they obtain an activation energy from an Arrhenius plot of  $\log \omega/T_M^{3/2}$  versus  $1/T_M$ . The model used by Losee<sup>17</sup> to find activation energies for deep levels also uses plots of  $\log \omega/T_M^{3/2}$  versus  $1/T_M$ , while Pautrat *et al.*<sup>18</sup> use plots of  $\log \omega/T_M^2$  versus  $1/T_M$  to obtain activation energies. Whether one plots the log of  $\omega$ ,  $\omega/T_M^{3/2}$ , or  $\omega/T_M^2$  to obtain activation energies depends on the particular model for carrier transport that is used. In general, the differences in numerical values of activation energy are small for the different ways of analyzing data. They are not adequate to explain the large differences in  $E_I$  for samples *A*–*C* compared to the values for samples *D* and *E*.

Impurity conduction in lightly doped semiconductors is characterized by a large decrease in resistivity for a relatively small increase in impurity concentration, the situation that occurs here. The conventional way of expressing the resistivity of a lightly doped semiconductor  $\rho$  is<sup>1</sup>

$$\rho = \rho_1 e^{\varepsilon_1/kT} + \rho_2 e^{\varepsilon_2/kT} + \rho_3 e^{\varepsilon_3/kT}, \quad (14)$$

where  $\varepsilon_1$ ,  $\varepsilon_2$ , and  $\varepsilon_3$  are activation energies for conduction in different regimes. The different conduction regimes are identified from plots of log of resistivity versus  $1/T$ .  $\varepsilon_1$  is the activation energy for freezeout of carriers from the valence (conduction) band onto ionized acceptors (donors).  $\varepsilon_2$  and  $\varepsilon_3$  are activation energies for different impurity conduction mechanisms at temperatures below which carrier freezeout occurs. Transport processes corresponding to  $\varepsilon_3$  are nearly always observed; processes corresponding to  $\varepsilon_2$  depend on compensation and are frequently not observed. The values of  $E_I$  for samples *A*–*C*, 17–23 meV, are those for freezeout and are related to  $\varepsilon_1$ . The values of  $E_I$  for samples *D* and *E* correspond to  $\varepsilon_2$  and  $\varepsilon_3$  and reflect impurity conduction in  $p$ -type GaAs.

Impurity conduction in lightly doped semiconductors depends on the overlap of the wave functions on neighboring donors or acceptors. The ratio of the mean distance between impurities  $r_S$  to the Bohr radius  $a_B^*$  determines different impurity conduction regimes. If  $N_M$  is the majority impurity,  $r_S = (4\pi N_M/3)^{-1/3}$  and  $a_B^* = 4\pi\epsilon_S\epsilon_0/mq^2$ , where  $\hbar$  is Planck's constant,  $m$  is the carrier effective mass, and  $q$  is the electron charge. For spherically symmetric, hydrogenic impurities, such as donors in GaAs, there is an unambiguous value of  $a_B^*$ . However, acceptors in GaAs are not spherically symmetric. At  $k=0$ , there are degenerate heavy-hole and light-hole bands with effective mass  $m_{\text{HH}} = 0.5m_0$  and  $m_{\text{LH}} = 0.08m_0$ , where  $m_0$  is the free-electron mass.<sup>35</sup> The corresponding values of Bohr radius are  $a_{\text{HH}}^* = 13 \text{ \AA}$

and  $a_{\text{LH}}^* = 83 \text{ \AA}$ . The situation is similar to that for impurity conduction in  $p$ -type Ge and  $p$ -type Si, which has been reviewed by Chroboczek.<sup>1</sup> The heavy-hole mass determines acceptor energies and densities of states but the light-hole mass determines impurity conduction and effects that depend on the overlap of wave functions at a distance from acceptors. For samples *A*–*C*,  $r_S/a_{\text{LH}}^* \sim 9.4$ , and for samples *D* and *E*,  $r_S/a_{\text{LH}}^* \sim 4.4$ . Both values of  $r_S/a_{\text{LH}}^*$  correspond to the low concentration regime for impurity conduction discussed by Chroboczek. The lower value of  $r_S/a_{\text{LH}}^*$  should give a single value of  $\epsilon_3$  at low temperatures.

The picture of conduction in lightly doped  $p$ -type GaAs that emerges is that isolated acceptors lie  $\sim 20$ – $23$  meV above the valence band. At concentrations of  $5 \times 10^{15} \text{ cm}^{-3}$  there is a well-defined activation energy for ac transport,  $\sim 6$  meV. This is not large enough for hole excitation into the valence band. However, it is not clear if this value corresponds to  $\epsilon_2$ , the energy separation of the upper Hubbard impurity band from the acceptor level, or whether it is the energy for activated hopping  $\epsilon_3$ . Measurements on samples with a wider concentration range are needed to tell if  $E_I$  is constant, and to determine the concentration at the metal-nonmetal transition. One measurement of the activation energy of conduction for a Be doping of  $2.2 \times 10^{18} \text{ cm}^{-3}$  also gave  $E \sim 5$  meV,<sup>10</sup> but it is a very long extrapolation from the same value of  $E_I$  measured at  $5 \times 10^{15} \text{ cm}^{-3}$  doping in the present work. The range of values of  $E_I$  for samples *A*–*C*, 17–23 meV, suggests that an impurity band begins to form for  $N_A - N_D < 10^{15} \text{ cm}^{-3}$ .

Hall measurements remain the method of choice to study impurity conduction, since the different conduction regimes are clearly delineated by the measurements. However, admittance measurements on capacitors offer some advantages for studying  $p$ -type GaAs or materials with  $E_A \gtrsim 0.020$  eV. Hall-effect measurements in  $p$ -type GaAs are not possible below  $\sim 30$  K because the Hall mobility drops abruptly and the sample resistance becomes too large. Admittance measurements are made in the temperature region below 30 K. This is possible be-

cause the critical dimension of the active region,  $0.6 \text{ }\mu\text{m}$ , is much smaller than the sample size of several hundred  $\mu\text{m}$ , which is used for Hall measurements on Hall bars or van der Pauw samples. Another advantage of  $\text{Al}_x\text{Ga}_{1-x}\text{As}$  capacitors for such studies is the ability to control substrate doping and compensation over wide ranges by independently varying the evaporation of  $p$ -type and  $n$ -type dopants during MBE.

In summary, the combination of  $C$ - $V$  measurements on  $p$ -type  $\text{Al}_x\text{Ga}_{1-x}\text{As}$  capacitors at fixed frequency and temperature with admittance measurements at fixed bias and variable temperature and frequency serves to determine two activation energies in  $p^-$ -type GaAs. The separation of the acceptor level from the valence band  $E_A$  is estimated from the temperature for the appearance of a GB dip in  $C$ - $V$  curves. The activation energy for ac transport in  $p^-$ -type GaAs,  $E_I$ , is determined from admittance measurements. Carrier freezeout and impurity conduction have been studied in two groups of  $p$ -type  $\text{Al}_x\text{Ga}_{1-x}\text{As}$  capacitors that differ in their substrate doping. Both groups of samples have lightly doped substrates. For one group,  $N_S \sim 5 \times 10^{14} \text{ cm}^{-3}$ ; for the other,  $N_S \sim 5 \times 10^{15} \text{ cm}^{-3}$ . For both groups,  $E_A \sim 20$  meV, which is somewhat smaller than the optical value for a Be acceptor in GaAs. For the lighter-doped samples,  $E_I = 17$ – $23$  meV, which agrees with  $E_A$  from  $C$ - $V$  measurements. For the heavier-doped samples,  $E_I \sim 5$ – $6$  meV; ac transport of holes is either through a well-defined impurity band separated by  $\sim 5$  meV from the energy level of an isolated acceptor and by  $\sim 15$ – $20$  meV from the valence band, or by activated hopping.

#### ACKNOWLEDGMENTS

Samples *A*–*C* were grown by H. Meier and samples *D* and *E* were grown by S. L. Wright. Capacitors were processed by K. Seo, P. M. Solomon, and F. Canora. This work would not have been possible without their efforts. I have benefited from conversations with N. Lipari, and with F. Stern, who also gave a critical reading of the manuscript.

<sup>1</sup>For a review, see J. A. Chroboczek, in *Noncrystalline Semiconductors*, edited by M. Pollak (CRC, Boca Raton, 1987), Vol. III, p. 109.

<sup>2</sup>B. I. Shklovskii and A. L. Efros, *Electronic Properties of Doped Semiconductors* (Springer-Verlag, Berlin, 1984).

<sup>3</sup>B. I. Shklovskii and A. L. Efros, *Fiz. Tekh. Poluprovodn.* **14**, 825 (1980) [*Sov. Phys. Semicond.* **14**, 487 (1980)].

<sup>4</sup>H. Fritzsche and M. Cuevas, *Phys. Rev.* **119**, 1238 (1960).

<sup>5</sup>H. Fritzsche, in *The Metal Non-Metal Transition in Disordered Systems*, edited by L. R. Friedman and D. P. Tunstall (S.U.S.S.P., Edinburgh, 1978), p. 193.

<sup>6</sup>J. A. Chroboczek, F. H. Pollak, and H. F. Staunton, *Philos. Mag.* **B 50**, 113 (1984).

<sup>7</sup>O. V. Emel'yanenko, T. S. Lagunova, D. N. Nasledov, D. D. Nedeoglo, and I. N. Timchenko, *Fiz. Tekh. Poluprovodn.* **7**, 1919 (1973) [*Sov. Phys. Semicond.* **7**, 1280 (1980)].

<sup>8</sup>H. Kahlert, G. Landwehr, A. Schlachetzki, and H. Salow, *Z. Phys. B* **24**, 361 (1976).

<sup>9</sup>F. Ermanis and K. Wolfstirn, *J. Appl. Phys.* **37**, 1963 (1966).

<sup>10</sup>J. A. Hutchby and K. V. Vaidyanathan, *J. Appl. Phys.* **48**, 2559 (1977).

<sup>11</sup>O. V. Emel'yanenko, T. S. Lagunova, and D. N. Nasledov, *Fiz. Tverd. Tela. (Leningrad)* **3**, 198 (1961) [*Sov. Phys. Solid State* **3**, 144 (1961)].

<sup>12</sup>M. Ilegems, *J. Appl. Phys.* **48**, 1278 (1977).

<sup>13</sup>N. Chand, R. Fischer, J. Klem, T. Henderson, P. Pearah, W. T. Masselink, Y. C. Chang, and H. Morkoç, *J. Vac. Sci. Technol.* **B 3**, 644 (1985).

<sup>14</sup>V. Swaminathan, J. L. Zilko, W. T. Tsang, and W. R. Wagner, *J. Appl. Phys.* **53**, 5163 (1982).

<sup>15</sup>P. K. Bhattacharya, H.-J. Bühlmann, M. Ilegems, and J. L. Staehli, *J. Appl. Phys.* **53**, 6391 (1982).

- <sup>16</sup>J. S. Blakemore, *Semiconductor Statistics* (Macmillan, New York, 1962), p. 130.
- <sup>17</sup>D. L. Losee, *J. Appl. Phys.* **46**, 2204 (1975).
- <sup>18</sup>J. L. Pautrat, B. Katircioglu, N. Magnea, D. Bensahel, J. C. Pfister, and L. Revoil, *Solid-State Electron.* **23**, 1159 (1980).
- <sup>19</sup>I. V. Marchishin, V. N. Ovsyuk, and S. B. Sevastianov, *Phys. Status Solidi A* **106**, 153 (1988).
- <sup>20</sup>S. Duenas, I. Izpura, J. Arias, L. Enriquez, and J. Barbolla, *J. Appl. Phys.* **69**, 4300 (1991).
- <sup>21</sup>E. H. Nicollian and J. R. Brews, *MOS (Metal Oxide Semiconductor) Physics and Technology* (Wiley, New York, 1982), p. 176.
- <sup>22</sup>J. Shewchun, V. Temple, and R. Clarke, *J. Appl. Phys.* **43**, 3487 (1972).
- <sup>23</sup>J. Shewchun, R. A. Clarke, and V. A. K. Temple, *IEEE Trans. Electron Devices* **ED-19**, 1044 (1972).
- <sup>24</sup>D. V. Lang, M. B. Panish, F. Capasso, J. Allam, R. A. Hamm, A. M. Sergent, and W. T. Tsang, *Appl. Phys. Lett.* **50**, 736 (1987).
- <sup>25</sup>S. Aymeloglu and J. N. Zemel, *IEEE Trans. Electron Devices* **ED-23**, 466 (1976).
- <sup>26</sup>T. W. Hickmott, *Solid State Commun.* **63**, 371 (1987).
- <sup>27</sup>T. W. Hickmott, P. M. Solomon, R. Fischer, and H. Morkoç, *J. Appl. Phys.* **57**, 2844 (1985).
- <sup>28</sup>J. Batey and S. L. Wright, *J. Appl. Phys.* **59**, 200 (1986).
- <sup>29</sup>T. W. Hickmott, *Phys. Rev. B* **38**, 12 404 (1988).
- <sup>30</sup>P. V. Gray and D. M. Brown, *Appl. Phys. Lett.* **13**, 247 (1968).
- <sup>31</sup>E. H. Nicollian and J. R. Brews, *MOS (Metal Oxide Semiconductor) Physics and Technology* (Ref. 21), p. 380.
- <sup>32</sup>T. W. Hickmott, *Phys. Rev. B* **40**, 11 683 (1989).
- <sup>33</sup>*C-V* curves at low temperature were calculated with a computer code provided by F. Stern. It is a continuum model that includes no quantum effects.
- <sup>34</sup>G. F. Neumark, *Phys. Rev. B* **5**, 408 (1972).
- <sup>35</sup>J. S. Blakemore, *J. Appl. Phys.* **53**, R123 (1982).